Multifractal analysis in reciprocal space and the nature of the Fourier transform of self-similar structures

1990 J. Phys. A: Math. Gen. 23 3769

(http://iopscience.iop.org/0305-4470/23/16/024)

J. Phys. A: Math. Gen. **23** (1990) 3769-3797. Printed in the UK

Multifractal analysis in reciprocal space and the nature of the Fourier transform of self-similar structures

C Godrèche† and J M Luck‡

† Service de Physique du Solide et de Résonance Magnétique, CEA, Saclay, 91191 Gif-sur-Yvette cedex, France

‡ Service de Physique Théorique (Laboratoire de l'Institut de Recherche Fondamentale du Commissariat à l'Energie Atomique), CEA, Saclay, 91191 Gif-sur-Yvette cedex, France

Received 26 February 1990

Abstract. We propose to use multifractal analysis in reciprocal space as a tool to characterise, in a statistical and global sense, the nature of the Fourier transform of geometrical models for atomic structures. This approach is especially adequate for shedding some new light on a class of structures introduced recently, which exhibit 'singular scattering'. Using the language of measure theory, the Fourier intensity of these models is presumably singular continuous, and therefore represents an intermediate type of order, between periodic or quasiperiodic structures, characterised by Bragg peaks (atomic Fourier transform), and amorphous structures, which exhibit diffuse scattering (absolutely continuous Fourier transform). This general approach is illustrated in several examples of self-similar one-dimensional squences and structures, generated by substitutions. A special emphasis is put on the relationship between the nature of the Fourier intensity of these models and the $f(\alpha)$ spectrum obtained by multifractal analysis in reciprocal space.

1. Introduction

In recent years we have investigated, mostly in collaboration with S Aubry [1-5], the nature of the diffraction spectra, or Fourier transforms, of some ordered distributions of matter on the line. These studies were motivated by the discovery of quasicrystals, by theoretical research into the nature of the ground states of complex incommensurate structures, and by the desire to put these two fields into perspective. The aim of this paper is to show that multifractal analysis gives some new insight into the nature of the Fourier transforms of such structures.

Multifractal analysis (see [6, 7] for reviews) is a tool for characterising, in a statistical sense, the nature of a positive measure. By definition, a positive measure describes how a positive quantity, such as mass, is distributed on a set, the support of the measure. This concept may be illustrated as follows. Take a can containing one unit of mass of paint, and spread it in some (possibly very irregular) fashion along a line. The mass-of-paint measure is a probability measure, since it is assumed to be normalised to unity. The total measure up to the point x on the line, denoted by $M(x)$, is also called the distribution function of the measure. It represents the mass already spread out up to x

$$M(x) = \int_{-\infty}^{x} \mathrm{d}\mu(x'). \tag{1.1}$$

In this paper, the analogue of the mass of paint is, e.g., the number of neutrons counted

0305-4470/90/163769+29$03.50

in a diffraction experiment (given by the Fourier intensity), and the support is reciprocal space, i.e. the space of wavevectors q. The Fourier intensity measure of a structure will be defined more precisely in section 3.

One distinguishes three pure types of positive measures.

(i) Atomic measures, such as the probability measure of the binomial law, obtained by tossing a coin repetitively, where the number of heads x assumes only a countable set of values. $M(x)$ is then a discontinuous staircase function (discontinuities take place at integer values of x in the example).

(ii) Absolutely continuous (AC) measures, such as the normal law, correspond to a differentiable function $M(x)$. The derivative $M'(x) = \rho(x)$ is the density of the measure (a Gaussian function in the example).

(iii) Singular continuous (SC) measures are much less known than the two previous classes. They are defined as the measures which have neither an atomic nor an AC component. For instance, the natural measure on the triadic Cantor set is SC. The associated function $M(x)$ is known as a devil's staircase. But the support of a SC measure can also be as smooth as the full real line, or an interval. This is for instance, the case of the two-scale Cantor measure based upon the binomial distribution (see [7] and references therein). Similarly, the SC Fourier measures studied in the following will always have the full q line as support.

The multifractal formalism describes in a global way the singular character of a probability measure. Let us recall briefly the main lines of this formalism. For the sake of simplicity, consider a probability measure supported by the unit interval $[0, 1]$, instead of the whole real axis. This interval is divided into $N = 1/\varepsilon$ boxes of size ε. The ith box bears a probability

$$p_i = \int_{i\varepsilon}^{(i+1)\varepsilon} \mathrm{d}\mu(x') \qquad i = 1, \ldots, N. \tag{1.2}$$

Thus p_i provides some information on the local behaviour of the measure around the point $x = i\varepsilon$. In particular, suppose that one has the power law

$$p_i \sim \varepsilon^{\alpha} \qquad \text{when } \varepsilon \to 0. \tag{1.3}$$

The exponent α gives an estimate of the strength of the local singularity of the measure at $x = i\varepsilon$. Let us summarise briefly which kinds of local behaviour can be expected in the three pure types of measures recalled above.

(i) For an AC measure, we have $p_i \approx \rho(x)\varepsilon$ when $\varepsilon \to 0$. Thus (1.3) holds, with $\alpha = 1$, provided the density $\rho(x)$ does not vanish.

(ii) For a discrete atomic measure, of the form $\Sigma_a\, q_a \delta(x - x_a)$, each box probability p_i is either zero, or equal to one of the q_a, for ε small enough. In the latter case, (1.3) still holds, with $\alpha = 0$.

(iii) Finally, for a SC measure there is no general rule. In principle, any value of the local exponent α may occur. It may turn out as well that no simple behaviour at all is obeyed.

The multifractal analysis is the appropriate tool for looking at the local singular behaviour of these types of measures, at least in a statistical sense that will become clear later on. The starting point of the analysis is the partition function, defined for any real number Q by

$$Z(Q) = \sum_{i=1}^{N} p_i^Q. \tag{1.4}$$

It is understood that the summation runs over non-empty boxes only ($p_i \neq 0$).

The measure $d\mu$ is said to be multifractal whenever one has the power-law (scaling) behaviour

$$Z(Q) \sim \varepsilon^{\tau(Q)} \tag{1.5}$$

Since $Z(1) = 1$ for any ε, because of normalisation, one has $\tau(1) = 0$. One is thus led to set

$$\tau(Q) = (Q-1)D_Q. \tag{1.6}$$

D_Q is referred to as the generalised (Rényi) dimension of index Q. For $Q = 0$, the partition function $Z(0)$ just counts the number of non-empty boxes of size ε. Thus D_0 is the Hausdorff, or fractal, dimension of the support of the measure. D_1 and D_2 are referred to as the information and correlation dimensions of the measure, respectively. In the case of a 'regular' fractal measure, such as the triadic Cantor measure, one has $D_Q = D_0$ for any Q. Regular fractals are thus characterised by one single dimensionality.

The usual interpretation of the existence of a continuous infinity of generalised dimensions D_Q is as follows. Assume that the values of x can be sorted according to their local exponent α, and that the set S_α of points x with a local exponent α has a dimension $f(\alpha)$. Once the measure is regularised at scale ε as explained above, one can argue that the number $N_\alpha(\varepsilon)$ of boxes such that the scaling law (1.3) holds, itself obeys a power law, namely

$$N_\alpha(\varepsilon) \sim \varepsilon^{-f(\alpha)}. \tag{1.7}$$

The partition function $Z(Q)$ can then be recast as an integral over the values of the exponent α

$$Z(Q) \sim \int d\alpha\, \varepsilon^{\alpha Q - f(\alpha)} \tag{1.8}$$

which is evaluated by the saddle-point method for $\varepsilon \to 0$. The condition that the exponent in (1.8) is stationary yields the value of Q, namely

$$Q = \frac{df}{d\alpha} \tag{1.9}$$

and the associated value of the exponent yields the quantity $\tau(Q)$

$$\tau(Q) = \alpha Q - f(\alpha). \tag{1.10}$$

The function $\tau(Q)$ is therefore obtained from $f(\alpha)$ by means of a Legendre transform. The inverse transform is given by

$$\alpha = \frac{d\tau}{dQ} \tag{1.11}$$

together with (1.10).

When the exponent Q varies continuously from $-\infty$ to ∞, the quantities α and $f(\alpha)$ defined by (1.10), (1.11) in terms of the exponent $\tau(Q)$ describe a continuous curve in the (α, f) plane, known as the $f(\alpha)$ spectrum. In virtue of (1.9), the slope of this curve is Q itself. The top of the curve is reached for $Q = 0$; the corresponding value of f is the dimension D_0 of the support, whereas the value α_0 of α is not known *a priori*. With respect to this maximum, the right (respectively left) part of the curve corresponds to negative (respectively positive) values of the index Q.

This long reminder of a well known formalism was necessary in order both to fix notation, and to underline the statistical nature of the information on a positive measure provided by its multifractal analysis. Let us recall that both atomic and AC measures

are expected to exhibit one single value of the local exponent α, namely $\alpha = 0$ and $\alpha = 1$, respectively, and therefore only SC measures should give rise to a non-degenerate $f(\alpha)$ spectrum.

As mentioned above, the measures considered hereafter are Fourier intensities of one-dimensional structures, the support of which is the entire real q line. We will study more precisely the Fourier spectra of substitutional sequences, generated by substitutions, or inflation rules in more physical terms. Our motivation in doing so is as follows. In the study of ordered structures it is important to disentangle the interplay between the types of order present in the structures, and the properties of their Fourier transforms. In this respect, substitutional sequences provide plenty of interesting test cases, in spite of their one-dimensional character. Substitutions also appear in the study of real structures. Indeed, the Fibonacci sequence is naturally met in the study of quasicrystals.

One of the questions raised in our previous works [4, 5] is the nature of the Fourier transforms of these sequences, or of the associated geometrical structures, as will be explained below. Just as any positive measure, the Fourier intensity of a structure may have three components, namely an atomic one (Bragg peaks), an AC one (diffuse scattering), and an SC one. In this paper we show how a multifractal analysis of the intensity measure, in particular through the $f(\alpha)$ curve, gives some information on the nature of the Fourier transform, especially concerning the presence or the absence of an AC component in the spectrum.

The organisation of this paper is as follows. Section 2 is devoted to a caveat, concerning the finite-size effects that are unavoidably met when coming to actual computations. We show on a simple example that numerical computations on finite samples, or with finite data series, may produce artefacts that could be taken for a real multifractal behaviour. We propose a way of getting around this problem, and define an accurate test of multifractality, that will be used systematically in the following. This criterion can certainly be useful in many other circumstances, where one is not sure *a priori* to deal with a multifractal measure. We recall in section 3 various useful definitions concerning substitutional sequences, as well as the basic notions of Fourier analysis. Section 4 is entirely devoted to the study of several examples of Fourier spectra associated with substitutional sequences, namely the well known Fibonacci sequence, two versions of the 'circle sequence' introduced in our previous studies [1-5], the Thue-Morse and Rudin-Shapiro arithmetic sequences, and finally two generic examples of sequences which do not have the PV property, to be described in subsection 3.3. In each case, the multifractal analysis of the Fourier intensity measure is compared with information available from other sources. A concise summary of this multifractal analysis in reciprocal space is presented in section 5.

2. Discussion of convergence properties

Since numerical computations necessarily deal with finite samples, and finite data series, a multifractal analysis may be plagued with artefacts coming from finite-size effects. The importance of such effects is illustrated in the following on a very simple and explicit example.

Let us consider the following distribution of weights (box probabilities)

$$p_i = \frac{2i}{N^2} \qquad i = 1, \ldots, N \tag{2.1}$$

which are normalised (to leading order in N). The associated partition function $Z(Q)$ is easily evaluated for large N by replacing the sum in the definition (1.4) by an integral. We obtain

$$Z(Q) \approx N^{1-Q} \frac{2^Q}{Q+1}. \tag{2.2}$$

Since N plays the part of $1/\varepsilon$ in the discussion of section 1, a blind usage of (1.5) leads to the estimate

$$\tau(Q) = Q - 1 + \frac{\phi(Q)}{\ln N} \qquad \text{with } \phi(Q) = \ln(Q+1) - Q \ln 2. \tag{2.3}$$

Hence $\tau(Q)$ is asymptotically equal to $Q-1$. As a consequence, α and $f(\alpha)$ are equal to 1 for all values of Q. The $f(\alpha)$ curve is thus degenerate, and reduces to one point, namely its top. This result could be expected since the weights defined by (2.1) correspond to an AC measure with support [0; 1]. With the notation of section 1, we have $\varepsilon = 1/N$, $x = i\varepsilon$, and $\rho(x) = 2x$. This distribution of weights has no multifractal character at all.

Nevertheless, it is striking to observe that, as long as N is finite, the data yield a seemingly $f(\alpha)$ curve, which is not reduced to one point. This artefact is clearly a finite-size effect.

This simple example leads us to emphasise a caveat: any seemingly multifractal $f(\alpha)$ curve might just be entirely due to finite-size effects. Two remarks are in order. The number N of data points enters the correction term in (2.3) through a logarithm. These effects are therefore dying off very slowly. Moreover, in any practical situation, the convergence is also affected by more or less random fluctuations, so that the $1/(\ln N)$ terms cannot be eliminated by simple convergence acceleration schemes, based, e.g., on subtractions.

We propose the following strategy to discriminate a real multifractal behaviour from a finite-size artefact. The idea consists in performing a careful local analysis of the $f(\alpha)$ curve in the vicinity of its top, which corresponds to $Q \to 0$. Indeed, the top of the curve obviously corresponds to the maximal value of f, and hence to the maximal number of boxes $N_\alpha(\varepsilon)$, by virtue of the estimate (1.7). This region is therefore expected to be the least affected by any fluctuation or finite-size effect. In a more quantitative way, consider the curvature of the $f(\alpha)$ curve at its top. Equations (1.9)-(1.11) imply that this quantity is given by

$$C = \left(\frac{\mathrm{d}^2 f}{\mathrm{d}\alpha^2}\right)_{\alpha=\alpha_0} = \left(\frac{\mathrm{d}^2 \tau}{\mathrm{d}Q^2}\right)^{-1}_{Q=0}. \tag{2.4}$$

The estimate (2.3) leads to

$$C \approx \frac{\ln N}{\phi''(0)} \tag{2.5}$$

i.e. $C \approx -\ln N$ in the present case. The curvatures of the seemingly $f(\alpha)$ curves corresponding to successive finite sizes diverge logarithmically with the number of data points. This divergence demonstrates that no smooth $f(\alpha)$ curve exists in the limit of an infinite system. In other words, as expected, the AC measure under consideration has no multifractal spectrum.

The evaluation of the curvature C will be done systematically for the various examples studied in the following. In some cases, extracting the full scaling function

$\phi(Q)$ may provide some additional information. Fortunately, in the examples that will be considered below, namely substitutional sequences, $\ln N$ will turn out to be a very natural variable.

These considerations can be extended to an arbitrary AC distribution on $[0; 1]$, given by its density $g(x)$. The normalised weights are

$$p_i = \frac{1}{Nm(1)} g(i/N) \qquad i = 1, \ldots, N \tag{2.6}$$

with the definition

$$m(Q) = \int_0^1 [g(x)]^Q \, dx \tag{2.7}$$

of the moment function. It is easily found that

$$Z(Q) \approx N^{1-Q} \frac{m(Q)}{m(1)^Q} \qquad N \to \infty. \tag{2.8}$$

Hence $\tau(Q)$ exhibits the very same scaling form as in (2.3), with

$$\phi(Q) = Q \ln m(1) - \ln m(Q). \tag{2.9}$$

We have in particular

$$\begin{aligned} -\phi''(0) &= m''(0) - m'(0)^2 \\ &= \int_0^1 \ln^2 g(x) \, dx - \left(\int_0^1 \ln g(x) \, dx \right)^2. \end{aligned} \tag{2.10}$$

The right-hand side is manifestly positive. Equation (2.10) thus yields a negative amplitude for the curvature C, once inserted into (2.5), as it should.

3. Substitutional sequences and structures, and their Fourier spectra

In this section we recall various definitions concerning substitutional sequences, and the associated structural models, as well as some generalities about their Fourier transforms.

3.1. Substitutional sequences and structures

A substitutional sequence is generated by a substitution σ acting on an alphabet, namely a finite number of letters $\{A, B, C, \ldots\}$. Let us illustrate this definition on the simple and well known example of the Fibonacci sequence. The Fibonacci sequence is perhaps the simplest of all self-similar structures. It can be viewed as the one-dimensional analogue of the two-dimensional Penrose tilings, and the three-dimensional tilings with, e.g., icosahedral symmetry, used as structural models for quasicrystals. In this simple case, the alphabet $\{A, B\}$ consists of two letters. By the substitution σ_F they are transformed according to the rule

$$\sigma_F \begin{cases} A \to B \\ B \to BA \end{cases} \tag{3.1}$$

We introduce the notation

$$A_n = \sigma_F^n(A) \qquad B_n = \sigma_F^n(B) \tag{3.2}$$

for the words obtained by acting n times with σ_F on the letters A and B.

It is easily realised that the words defined in (3.2) obey the following recursion:

$$A_{n+1} = B_n \qquad B_{n+1} = B_n A_n. \tag{3.3}$$

The words B_n can be eliminated from (3.3). We obtain thus a three-term recursion relation for the A_n, namely

$$A_{n+2} = A_{n+1} A_n. \tag{3.4}$$

This last property is a peculiarity of the Fibonacci substitution, which will not hold in general. We will therefore stick to the general formalism, using two letters.

Let us denote by ν_n^A and ν_n^B the total numbers of letters contained in the words A_n and B_n. In order to evaluate these numbers, it is advantageous to introduce the matrix **M** of the substitution, usually defined as

$$\mathbf{M} = \begin{pmatrix} \text{number of } A \text{ in } A_1 & \text{number of } A \text{ in } B_1 \\ \text{number of } B \text{ in } A_1 & \text{number of } B \text{ in } B_1 \end{pmatrix}. \tag{3.5}$$

In the present case, this definition yields

$$\mathbf{M} = \begin{pmatrix} 0 & 1 \\ 1 & 1 \end{pmatrix}. \tag{3.6}$$

The numbers of letters introduced above obey the recursion relation

$$\begin{pmatrix} \nu_{n+1}^A \\ \nu_{n+1}^B \end{pmatrix} = \mathbf{M}^t \begin{pmatrix} \nu_n^A \\ \nu_n^B \end{pmatrix} \tag{3.7}$$

with the initial conditions $\nu_0^A = \nu_0^B = 1$, and where $\mathbf{M}^t$ denotes the transpose of the matrix **M**.

We are thus led to evaluate the successive powers of the substitution matrix. In the present case, we have

$$\mathbf{M}^n = \begin{pmatrix} F_{n-1} & F_n \\ F_n & F_{n+1} \end{pmatrix} \tag{3.8}$$

where the Fibonacci numbers are defined by

$$F_n = F_{n-1} + F_{n-2} \qquad \text{with } F_0 = 0,\ F_1 = 1. \tag{3.9}$$

We are thus left with

$$\nu_n^A = F_{n+1} \qquad \nu_n^B = F_{n+2}. \tag{3.10}$$

The Fibonacci numbers are deeply connected with the golden mean $\tau = \frac{1}{2}(1+\sqrt{5})$. We have in particular

$$F_n = \frac{1}{\sqrt{5}} [\tau^n - (-\tau^{-1})^n]. \tag{3.11}$$

This last identity is clearly related to the fact that the eigenvalues of the matrix **M** are τ and $-\tau^{-1}$.

When the generation label n becomes large, the words A_n converge to the infinite Fibonacci sequence. From the infinite sequence of letters, one may build two different objects, hereafter called the abstract sequence and the structural model.

(i) In the case of the abstract sequence, the letters A and B are interpreted as numbers, according to some correspondence rule, such as e.g.

$$A: \varepsilon = 1 \qquad B: \varepsilon = -1 \tag{3.12}$$

or any other choice. With the kth letter of the infinite sequence is thus associated a number ε_k. The abstract sequence, the Fourier transform of which will be considered in the following, is just the infinite sequence of numbers $\{\varepsilon_k\}$.

(ii) In the case of the structural model, with the letters A and B are associated two real numbers, to be interpreted as bond lengths (l_A, l_B), according to

$$A: l_A = 1 + \xi \qquad B: l_B = 1 \tag{3.13}$$

where the dimensionless parameter ξ measures how inhomogeneous, i.e. how far from periodic, the structure is. A one-dimensional geometrical structure is generated by putting atoms on a line, each pair of neighbouring atoms being separated by a bond length l_A or l_B, according to the sequence of letters. Hence the object, the Fourier transform of which will be considered in the following, is the atomic density

$$\rho(x) = \sum_k \delta(x - u_k) \tag{3.14}$$

where u_k is the position of the kth atom on the line ($u_k - u_{k-1} = l_A$ or l_B; $u_0 = 0$).

For the structural model, the lengths of the finite structures associated with the words A_n and B_n are denoted by l_n^A and l_n^B, respectively. These lengths obey the same matricial recursion relation as the numbers of letters, namely

$$\begin{pmatrix} l_{n+1}^A \\ l_{n+1}^B \end{pmatrix} = \mathbf{M}^{\mathrm{t}} \begin{pmatrix} l_n^A \\ l_n^B \end{pmatrix} \tag{3.15}$$

with the initial values $l_0^A = l_A$ and $l_0^B = l_B$. We therefore have

$$l_n^A = F_{n-1} l_A + F_n l_B \qquad l_n^B = F_n l_A + F_{n+1} l_B. \tag{3.16}$$

The mean interatomic distance a is defined, by comparing (3.10), and (3.16), as the limit

$$a = \lim_{n\to\infty} \frac{l_n^A}{F_{n+1}} = \lim_{n\to\infty} \frac{l_n^B}{F_{n+2}} = \tau^{-2} l_A + \tau^{-1} l_B. \tag{3.17}$$

It is easy to check that the following differences, which have been evaluated by means of (3.11):

$$l_{n-1}^B - F_{n+1} a = l_n^A - F_{n+1} a = (l_B - l_A)(-\tau^{-1})^{n+1} \tag{3.18}$$

go to zero in the $n \to \infty$ limit. This last property is related to the existence of an average lattice [1-3]. As will be explained below, it is also related to the nature of the Fourier spectrum of the structure.

3.2. *Fourier transforms and intensity measures*

We now summarise some basic concepts of Fourier analysis. Let us denote by g_n^A the Fourier amplitudes of the abstract sequence, and by G_n^A those of the structural model,

associated in both cases with the words A_n. We have by definition

$$g_n^A(q) = \sum_{k=1}^{N} \varepsilon_k \, e^{-iqk} \tag{3.19a}$$

$$G_n^A(q) = \sum_{k=1}^{N} e^{-iqu_k} \tag{3.19b}$$

where $N = \nu_n^A$ is the number of letters in the word A_n.

The structure factors, or intensities, associated with these amplitudes are defined as

$$S_n^A(q) = \frac{1}{N} |g_n^A(q)|^2 \qquad \text{or} \frac{1}{N} |G_n^A(q)|^2. \tag{3.20}$$

Here and throughout this section, for the sake of simplicity, we prefer to use the generic notation $G_N(q)$ and $S_N(q)$ for the quantities defined above, using as a subscript N, the sample size, namely the number of terms in the Fourier sums, or the number of atoms.

When N becomes large, the intensities $S_N(q)$ may have very bad convergence properties (see below). In any case, from a rigorous viewpoint, the only well defined concept attached to the Fourier spectrum of the infinite sequence (or structure) is its intensity measure. This positive measure is defined by considering the distribution function, or integrated intensity

$$H(q) = \lim_{N \to \infty} \int_0^q S_N(q') \, dq'. \tag{3.21}$$

This quantity, analogous to $M(x)$ in (1.1), is well behaved in any circumstance. The intensity $S(q)$ of the infinite sequence (or structure), defined formally by

$$dH(q) = S(q) \, dq \tag{3.22}$$

has thus to be understood as a generalised function, or distribution.

Going back to a finite sample having N atoms, one can distinguish four possible kinds of local behaviour of the Fourier intensity, according to the growth of the amplitude $G_N(q)$ as a function of N.

(i) Bragg peaks. These are values q_0 of q such that

$$G_N(q_0) \approx C(q_0) N \tag{3.23}$$

$C(q_0)$ being some complex amplitude. $H(q)$ has then a discontinuity of strength $|C(q_0)|^2$ at $q = q_0$, and the structure factor $S(q)$ contains a delta function $|C(q_0)|^2 \delta(q - q_0)$. For periodic, and quasiperiodic (almost periodic) structures, the whole intensity is concentrated in Bragg peaks. In the language reviewed in section 1, these Fourier intensity measures are atomic.

(ii) Diffuse scattering. This situation corresponds to the structure factor $S(q)$ being a smooth function. This is, for instance, the case generically in amorphous structures, for which the Fourier amplitude $G_N(q)$ grows typically as $N^{1/2}$. The associated Fourier intensity measure is then AC (absolutely continuous).

(iii) Singular scattering. Suppose that one has for some wavevector q_0 the power law

$$G_N(q_0) \sim N^{\gamma} \qquad \text{with } \tfrac{1}{2} < \gamma < 1. \tag{3.24}$$

We have then $S_N(q_0) \sim N^{2\gamma - 1}$. Moreover, a finite-size scaling argument shows that, for $q \to q_0$ and N large, $S_N(q)$ is a function of the product $N(q - q_0)$ only. This observation leads to the following prediction:

$$|H(q) - H(q_0)| \sim |q - q_0|^{\alpha} \qquad \text{with } \alpha = 2(1 - \gamma) \tag{3.25}$$

concerning the integrated intensity of the infinite structure. The local exponents α and γ depend on q_0 *a priori*. Equation (3.25) is clearly very reminiscent of (1.3). Since $0<\alpha<1$, the intensity $S(q_0)$, which is formally equal to the derivative of $H(q)$ at q_0, is divergent, but 'less infinite' than in the presence of a Bragg peak, which corresponds formally to $\gamma=1$ ($\alpha=0$). It has been shown explicitly [5], for the example of a structure generated by a circle map, to be described in section 4.2, that the behaviour (3.25) holds around a dense set of values of the wavevector. In that case, γ depends indeed on q_0. The Fourier intensity measure in conjectured to be SC (singular continuous).

(iv) Finally, it may turn out that the Fourier amplitude $G_N(q)$ obeys no simple behaviour at all, considered as a function of the sample size. We suspect that, in the case of SC Fourier transforms, generic values of the wavevector do fall into this last class.

This last remark motivates our quest for a statistical study of the behaviour of the Fourier amplitude, as a function of the sample size N and of the wavevector q, which is precisely provided by the multifractal analysis described below.

Before going into this study, we should mention that a simpler version of such a statistical and global approach of the behaviour of the Fourier spectrum has been introduced for the first time in [4], where the following integral was considered:

$$I_N=\int_0^{q_{\max}} \mathrm{d}q\,|S_N(q)|^{1/2} \tag{3.26}$$

with, e.g., $q_{\max}=2\pi/a$, where a is the mean interatomic distance. From a heuristic viewpoint, the behaviour of this integral depends on the nature of the Fourier spectrum (intensity measure). More precisely the behaviour is as follows.

(a) If the Fourier spectrum is atomic, i.e. made of Bragg peaks, the integral I_N should fall off as $N^{-1/2}$. This law can be checked explicitly for periodic structures (up to logarithms).

(b) If the spectrum is absolutely continuous, i.e. if $S(q)$ is a smooth function, I_N should go to the constant limit $I=\int_0^{q_{\max}} \mathrm{d}q\,|S(q)|^{1/2}$, with increasing N.

(c) If the spectrum is singular continuous, one might suspect an intermediate kind of dependence of I_N on the sample size, like, e.g., $I_N\sim N^{-\beta}$, with $0<\beta<\frac{1}{2}$. Such a non-trivial power-law behaviour has indeed been observed numerically in [4], in the example mentioned above. This discovery was one of the motivations of the present study. As a matter of fact, the multifractal analysis found hereafter is a systematic generalisation of that approach. Indeed, the exponent β discussed above will be related in subsection 4.2 to the Rényi dimension $D_{1/2}$.

3.3. *Recursion relations between Fourier amplitudes, and consequences*

Let us now come back to the particular case of the substitutional sequences and structures described above, illustrating again the definitions on the example of the Fibonacci substitution. A natural way of evaluating the Fourier amplitudes of self-similar sequences (or structures), for both analytical and numerical purposes, is provided by deriving recursion relations between amplitudes associated with finite words. Such relations are a mere consequence of recursion relations (3.3) between the words themselves. We have thus

$$g^A_{n+1}=g^B_n \qquad g^B_{n+1}=g^B_n+\exp(-\mathrm{i}q\nu^B_n)g^A_n \tag{3.27a}$$

$$G^A_{n+1}=G^B_n \qquad G^B_{n+1}=G^B_n+\exp(-\mathrm{i}ql^B_n)G^A_n \tag{3.27b}$$

according to whether we look at the Fourier transform of the abstract sequence itself, or at the transform of the structural model. In the case of the Fibonacci sequence, the alternative form (3.4) yields a three-term recursion relation for the Fourier amplitudes corresponding to the words A_n alone, namely

$$g^A_{n+2}(q) = g^A_{n+1}(q) + \exp(-iq\nu^A_{n+1}) g^A_n(q) \tag{3.28a}$$

$$G^A_{n+2}(q) = G^A_{n+1}(q) + \exp(-iql^A_{n+1}) G^A_n(q). \tag{3.28b}$$

By virtue of (3.12, (3.13), the initial conditions for the above formulae are

$$g^A_0 = e^{-iq} \qquad g^B_0 = -e^{-iq} \tag{3.29a}$$

$$G^A_0 = \exp(-iql_A) = \exp[-iq(1+\xi)] \qquad G^B_0 = \exp(-iql_B) = e^{-iq}. \tag{3.29b}$$

Relations such as (3.27) will be used extensively as an efficient way of evaluating the Fourier amplitudes numerically, and the weights p_i appearing in the multifractal formalism (see subsection 3.4). The relations given above also permit one to obtain in a rigorous way some information on the local behaviour of the Fourier amplitudes.

Indeed, in the context of one-dimensional structural models generated by substitutions or, in the language of physicists, by inflation rules, the general question 'which substitutions give rise to an atomic Fourier spectrum?' has been addressed by Bombieri and Taylor (BT) [8], who have shown that, generically, a necessary and sufficient condition for the presence of an atomic component (i.e. Bragg peaks) in the Fourier spectrum is that the substitution have the PV (Pisot-Vijayaraghavan) property, defined as follows.

Consider an arbitrary substitution σ, acting on p letters. The PV property has to do with the eigenvalues of the associated matrix **M**. These eigenvalues are the p zeros of the characteristic polynomial $P(\lambda) = \det(\lambda \mathbf{1} - \mathbf{M})$. Assume that P is irreducible over the integers, i.e. cannot be written as the product of two polynomials with integer coefficients. Since **M** has non-negative entries, the Perron-Frobenius theorem states that the largest eigenvalue λ_1 is real and larger than unity. By definition, the substitution σ is said to have the PV property, and the number λ_1 is said to be a PV number, if all other eigenvalues $\lambda_2, \ldots, \lambda_p$ are smaller than unity in modulus. With the above assumption of irreducibility, the PV property is unambiguously attached to the algebraic integer λ_1, since the other $(p-1)$ eigenvalues are its algebraic conjugates.

Let us illustrate first how the argument works on the example of the Fibonacci sequence. It is well known that this structure is quasiperiodic, and thus has a purely atomic spectrum. This property may be shown by several approaches, in particular by using the cut and project method. In the present context, we can assert that, if the Fourier intensity contains a Bragg peak for the value q_0 of the wavevector q, then $G^A_n(q_0)$ has to grow linearly with the sample size, namely

$$G^A_n(q_0) \approx C(q_0) F_{n+2}. \tag{3.30}$$

This maximal growth is only obtained when the phase factor in (3.28b) goes asymptotically to unity in the $n \to \infty$ limit. This condition is equivalent to

$$\frac{q}{2\pi} l^A_n \to 0 \mod 1. \tag{3.31}$$

Using equations (3.16), (3.17), one finds that the values of q fulfilling the condition (3.31) are given by (see e.g. appendix B of [5] for an elementary proof)

$$\frac{qa}{2\pi} = j + k\tau \tag{3.32}$$

where j and k are arbitrary integers, and τ is the golden mean. These values of q correspond to the Bragg peaks of the model. The quasiperiodic nature of the Fibonacci chain is thus recovered. On the other hand, the substitution matrix **M**, given in (3.6), has a characteristic polynomial $P(\lambda) = \lambda^2 - \lambda - 1$, and eigenvalues $\lambda_1 = \tau$ and $\lambda_2 = -\tau^{-1}$. The Fibonacci substitution thus has the PV property.

More generally, BT have shown that, when the largest eigenvalue λ_1 of a substitution is a PV number, the Fourier spectrum of the associated structure has generically an atomic component. This result basically relies on the following theorem, due to Pisot [9]. If

$$x\theta^n \to 0 \mod 1 \tag{3.33}$$

for some real numbers x and θ, with θ greater than unity, then θ is a PV number, and x belongs to some module over the integers, related to θ in a known fashion.

Another way of realising the importance of the subleading eigenvalues of the substitution matrix **M** is to consider the differences evaluated in (3.18) in the case of the Fibonacci chain. For a generic substitution, it is easily seen that these differences behave as $|\lambda_2|^n$, where λ_2 denotes the second largest eigenvalue. If $|\lambda_2|$ is less that unity, the differences go to zero as $n \to \infty$, and the structure has a bounded fluctuation with respect to an average lattice. Conversely, if $|\lambda_2|$ is larger than unity, the density fluctuation of the structure diverges with the sample size as N^δ, where the fluctuation exponent is

$$\delta = \frac{\ln|\lambda_2|}{\ln \lambda_1}. \tag{3.34}$$

See [10] for a detailed study of this question.

Let us end this section with a word of caution. The BT argument does not imply that the Fourier intensity measure is purely atomic in the case of a substitution with the PV property. In other words, it does not rule out the presence of a continuous (either AC or SC) component in the Fourier spectrum. But, from a heuristic viewpoint, mixed Fourier spectra are expected to be rather exceptional.

3.4. Multifractal analysis of Fourier intensities

In order to use the multifractal formalism, the essential ingredient is the definition of the probability weights p_i. A straighforward use of the formalism recalled in section 1 would require the evaluation of the exact integrals of the intensity measure $\mathrm{d}H(q)$ characteristic of the infinite sequences (or structures), over small segments of length ϵ in q space. This procedure, which would need infinite computer time, is to be replaced by a carefully chosen approximate scheme.

The recursion relations derived above provide the appropriate tool for doing so. Indeed, rather than partitioning q space into boxes, we choose to consider periodic approximants of the infinite sequences (or structures), obtained by repeating infinitely many times the finite words A_n. The contact between both approaches can be made via general finite-size scaling arguments.

Consider first the Fourier transform of an abstract sequence. Let A_n be the finite word generated by acting n times with a substitution σ on the letter A. We build an infinite sequence by repeating this word in a periodic way. Let $N = \nu_n^A$ be the number of letters in this word. It is well known that the Fourier transform of the periodic

sequence consists of Bragg peaks, located at equally spaced wavevectors, of the form

$$q_m = \frac{2\pi m}{N} \tag{3.35}$$

where m runs over the integers. The associated amplitudes are, with the notation of subsection 3.2:

$$C_m = \frac{g_n^A(q_m)}{N}. \tag{3.36}$$

The Fourier amplitudes defined by (3.19a) are manifestly periodic functions of q, with period 2π. We can therefore restrict the analysis to one period in reciprocal space (i.e. one Brillouin zone), and consider only the wavevectors corresponding to $m = 1, \ldots, N$.

The weights that will enter the multifractal analysis are taken equal to the associated intensities, so normalised as to build up a probability measure, namely

$$p_m = \frac{|C_m|^2}{S} \qquad \text{with } S = \sum_{m=1}^{N} |C_m|^2. \tag{3.37}$$

We turn now to the analysis of the Fourier transform of a structural model generated by a substitution σ. We use the above procedure, namely repeating the finite structures associated with the words A_n. The main difference lies in the fact that the length $L = l_n^A$ of the structure is no longer an integer, and that the associated Fourier amplitude has no more periodicity in q space. The Bragg peaks are now located at

$$q_m = \frac{2\pi m}{L} \tag{3.38}$$

where m runs over the integers, and the associated amplitudes are

$$C_m = \frac{G_n^A(q_m)}{N}. \tag{3.39}$$

For obvious practical reasons, instead of considering the whole real q axis, we are bound to work with a finite number M of wavevectors. In the present case, there is some arbitrariness in the choice of M. In numerical calculations, we have chosen $1 \leqslant m \leqslant M$, with $M = zN$, and typically $z = 1$-5, so that the investigated wavevectors range from $q = 0$ to $q_{\max} \approx z(2\pi/a)$, since $L \approx Na$, where a denotes the mean interatomic distance. z is thus the number of 'Brillouin zones' that are studied.

Equipped with the above definitions of the p_i, we can use the formalism recalled in section 1 to evaluate the $f(\alpha)$ curve associated with any finite sample. The only technicality worth mentioning is that numerical differentiation can be avoided. Indeed, the derivatives of the partition function WRT Q can be evaluated directly as follows:

$$\begin{aligned} Z'(Q) &\equiv \frac{\mathrm{d}Z}{\mathrm{d}Q} = \sum_{i=1}^{M} p_i^Q \ln p_i \\ Z''(Q) &\equiv \frac{\mathrm{d}^2Z}{\mathrm{d}Q^2} = \sum_{i=1}^{M} p_i^Q (\ln p_i)^2. \end{aligned} \tag{3.40}$$

The values of α and f are then simply given by

$$\alpha = -\frac{Z'(Q)}{Z(Q)\ln M} \qquad f = \frac{1}{\ln M}\left(\ln Z(Q) - \frac{QZ'(Q)}{Z(Q)}\right) \tag{3.41}$$

and the curvature C of the $f(\alpha)$ curve at its top has the form

$$\frac{1}{C}=\frac{1}{\ln M}\left(\frac{Z'(0)^2}{Z(0)^2}-\frac{Z''(0)}{Z(0)}\right). \tag{3.42}$$

In (3.41), (3.42), M denotes the number of wavevectors involved in the analysis. We have the estimate

$$\ln M \approx n \ln \lambda_1 \qquad n \to \infty \tag{3.43}$$

where λ_1 denotes the Perron-Frobenius eigenvalue of the substitution.

It will become clear in section 4 that the most subtle point resides in the extrapolation of the data to the thermodynamic limit of an infinite sequence (or structure).

We end this section by discussing the interpretation of the $f(\alpha)$ spectrum associated with a Fourier transform. Besides the general aspects discussed in section 1, the following points are worth a comment.

(a) The abscissa α_0 of the top of the $f(\alpha)$ curve, corresponding to $Q=0$, is to be interpreted as the exponent characterising the local singularity of the intensity measure at a generic value of the wavevector q, i.e. *the strength of a generic singularity.* We have $\alpha_0 > 1$ whenever the intensity measure is a genuine multifractal. The associated value of f is equal to unity, since the support of the Fourier transform is the whole q axis in any circumstance.

(b) The extremal values $\alpha_{\min}$ and $\alpha_{\max}$ of the abscissa of the $f(\alpha)$ curve represent the minimal and maximal values of the singularity exponent α that occur with a 'reasonable' weight in reciprocal space. Subsection 4.2 will deal with an example where it has been shown explicitly that a countable set of wavevectors exhibit a local exponent $\alpha < \alpha_{\min}$.

(c) The value α_1, obtained for $Q=1$, obeys the relations $f(\alpha_1)=\alpha_1=D_1$, with the notation of section 1. This quantity is referred to as the *information dimension* of the Fourier intensity measure, or sometimes just as the dimension of the measure. Its distance to unity is a faithful measurement of how singular the Fourier transform is.

(d) The value $d_P=f(1)$, corresponding to $\alpha=1$, represents the dimension of the set of wavevectors q for which the local singularity exponent α is less than unity. In more physical terms, d_P represents thus *the dimension of the set of peaks* (in the general sense of singular scattering peaks, defined in subsection 3.2). This quantity is therefore,

Table 1. Summary of the multifractal analysis of the Fourier intensity measure of the sequences and structures considered in section 4. For each example, we give the nature of the Fourier intensity, whether it is a multifractal measure or not, and list the numerical values of some quantitative characteristics, described in subsection 3.4. Symbols are as follows: (1) conjectured result, (2) conjectured exact value, (3) conjectured exact value given in (4.27).

Sequence	FT	Multifractality	α_0	$\alpha_{\min}$	$\alpha_{\max}$	α_1	d_P
Fibonacci	QP	no	$2^{(2)}$	—	—	—	0
Circle (abstract)	QP	no	$2^{(2)}$	—	—	—	0
Circle (structure)	SC$^{(1)}$	yes	1.60	0.15	3.8	0.55	0.86
Thue-Morse	SC	yes (partial)	$2^{(2)}$	$0.41^{(3)}$	—	0.73	0.89
Rudin-Shapiro	AC	no	1	—	—	—	—
Binary non-PV	SC$^{(1)}$	yes (partial)	$2^{(2)}$	0.15	—	0.44	0.83
Ternary non-PV	SC$^{(1)}$	yes	1.36	0.2	3.6	0.64	0.92

at least in principle, accessible to experiment, via a careful box-counting type of data analysis.

These quantitative characteristics provided by the multifractal analysis of a Fourier transform are listed in table 1, and commented on in the conclusion, for each example studied in section 4.

4. Examples

In this section we present a detailed study of the statistical properties of the Fourier transforms of various one-dimensional self-similar sequences and structures, generated by substitution, using the multifractal formalism described above.

4.1. The Fibonacci sequence

The Fibonacci sequence has already been defined in section 3, where it was used extensively to illustrate various concepts and definitions associated with substitutional sequences and structures.

It is well known that the Fibonacci sequence is quasiperiodic. More precisely, the Fourier intensity $S(q)$ of the abstract Fibonacci sequence consists of delta functions, i.e. Bragg peaks, located at values of the wavevector q of the form

$$q = 2\pi(j + k\tau) \tag{4.1}$$

where j and k are two arbitrary integers, and τ denotes the golden mean, defined in subsection 3.1. The intensities of the Bragg peaks are

$$A_k = |C_k|^2 = \begin{cases} \sin^2(k\pi\tau)/(k\pi)^2 & \text{for } k \neq 0 \\ \tau^{-4} & \text{for } k = 0. \end{cases} \tag{4.2}$$

The binary structural model, constructed from the Fibonacci sequence by putting short and long bonds on a line, according to (3.13), has a very similar Fourier transform, with Bragg peaks still given by (4.1), where q is replaced by the product qa, with a being the mean interatomic distance, defined in (3.17).

This first example is therefore a test case for the multifractal analysis of a Fourier intensity, since the answer to the key question, namely the nature of the Fourier transform, is known from other approaches. Since the Fourier transform is quasiperiodic, we expect that the Fourier intensity measure is not multifractal. However, since the coefficients C_k of (4.2) exhibit a very slow fall-off, some anomalous convergence properties could be suspected.

The Fourier amplitudes $g_n^A(q)$ and $g_n^B(q)$ of the abstract Fibonacci sequence, and the amplitudes $G_n^A(q)$ and $G_n^B(q)$ of the binary structural model, corresponding to the successive iterates of the letters A and B, are easily obtained from the recursion relations (3.27), with the initial values (3.29).

In order to test the multifractality of the Fourier intensity, or rather its lack of multifractality, we have employed the curvature C of the $f(\alpha)$ curve at its top, defined by (2.4). Figure 1 shows this quantity, evaluated for the words A_n, plotted against the generation label n, for both the abstract sequence (lower data) and the structural model (upper data). In the latter case, the number z of 'Brillouin zones' defined in subsection 3.4 is equal to 1. The parameter ξ entering the definition of bond lenths is $\xi = -\tau^{-2}$,

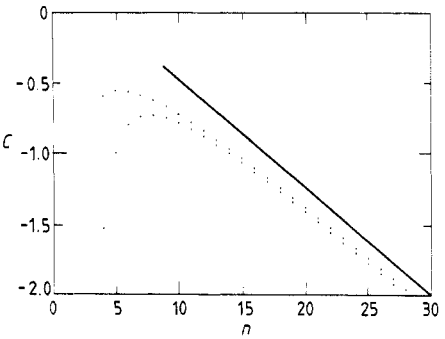

Figure 1. Plot of the curvature C of the apparent $f(\alpha)$ curves of the abstract Fibonacci sequence (lower data), and the associated structural model (upper data), against the generation label n. The straight line with slope $s \approx -0.073$ is meant as a guide for the eye.

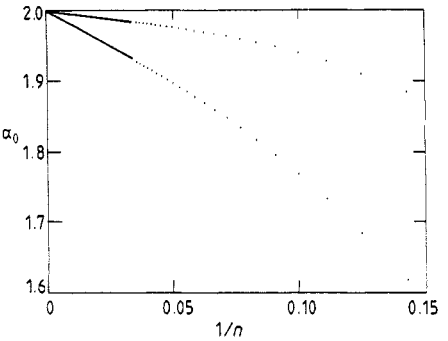

Figure 2. Plot of the abscissa α_0 of the top of the apparent $f(\alpha)$ curves of the Fibonacci sequence, against the reciprocal of the generation label n. Both the lower data (abstract Fibonacci sequence) and the upper data (structural model) converge linearly to the limit $\alpha_0 = 2$.

so that the ratio of both bond lengths be $l_B/l_A = \tau$, corresponding to the usual representation of the Fibonacci chain. In any case, we have checked that the results presented here do not depend in a sensitive way on the choice of ξ.

The last data points correspond to $n = 28$, i.e. $F_{29} = 514\,229$ letters or atoms, and as many values of q. Both series of data are clearly asymptotically linear for large n, with a common slope $s \approx -0.073$, shown as a full line on the plot. Hence the curvature C diverges linearly with the generation number, just as for the simple example studied in section 2. The $f(\alpha)$ curves of finite samples therefore become singular as their size grows, and the limit measure, namely the Fourier intensity of the infinite chain, is not multifractal.

Some aspects of the apparent $f(\alpha)$ curves associated with the finite words A_n can nevertheless be characterised in a quantitative way. The values of α_0, corresponding to the top of the $f(\alpha)$ curves, are plotted on figure 2, against $1/n$, up to $n = 28$, where n denotes the generation label, for both the abstract sequence (lower data) and the structural model (upper data). A linear convergence toward the limit $\alpha_0 = 2$ shows up rather clearly in both cases. As a matter of fact, this simple limit value can be explained by means of the following heuristic argument. Remember that α_0 is to be interpreted as the generic value of the singularity exponent α observed, at least in some statistical sense, for almost all values of q.

Consider a generic value q_* of q, and set $x_* = q_*/(2\pi)$. From a heuristic viewpoint, the behaviour of the distribution function $H(q)$ around q_* is dominated by the Bragg peaks of (4.1) that lie closest to $q = q_*$. The problem is thus to approximate a generic number x_* by numbers of the form $x_{j,k} = j + k\tau$. We do not aim at dealing with this problem in fully rigorous terms. For the case under consideration, it has been argued, e.g. in [5, 11, 12], that the answer is simple for some specific values of x_*, such as $x_* = \frac{1}{2}$. More precisely, this particular value, that will play an important role in subsection 4.2, has a regular infinite sequence of best approximants x_{j,k_L} labelled by an integer $L \geqslant 1$. We have $k_L = \frac{1}{2}F_{3L}$, and $\Delta x = |x_{j,k_L} - x_*| \sim \tau^{-3L} \sim 1/k_L$. Hence the largest Bragg peak that is close to $x_* = \frac{1}{2}$ within a distance Δx has an intensity $A \sim 1/k_L^2 \sim (\Delta x)^2$, in virtue of (4.2). Under the reasonable assumption that this gives the correct scaling for the total measure $\Delta H \equiv H(q_* + 2\pi\Delta x) - H(q_*)$, we finally obtain

$\Delta H \sim (\Delta x)^2$, whence the local singularity exponent $\alpha = 2$ for $q_* = \pi$. We now formulate the hypothesis that the scaling behaviour demonstrated here remains correct, in a statistical sense, for generic values of the wavevector. Thus the value $\alpha_0 = 2$ shows up in a natural way.

We have also studied the form of the apparent $f(\alpha)$ curves, in the vicinity of their top, and for large values of the generation label n. In analogy with the scaling behaviour (2.3) derived analytically in the case of the simple example considered in section 2, we hypothesise the following scaling form;

$$\tau(Q) \approx 2Q - 1 + \frac{\Phi(Q)}{n} \qquad n \to \infty. \tag{4.3}$$

Figure 3 shows a plot of the scaling amplitude $\Phi(Q)$ against Q, in the case of the abstract Fibonacci sequence. The data were obtained by taking (4.3) as a strict equality for large enough values of n ($18 \leqslant n \leqslant 28$). In particular, by taking the derivative of (4.3) at $Q = 0$, we obtain

$$\alpha_0 \approx 2 + \frac{\Phi'(0)}{n}. \tag{4.4}$$

Indeed, the slope $\Phi'(0) \approx -2.1$ of the plot of figure 3 at the origin agrees with the slope of the lower curve of figure 2, which shows a plot of α_0 against $1/n$.

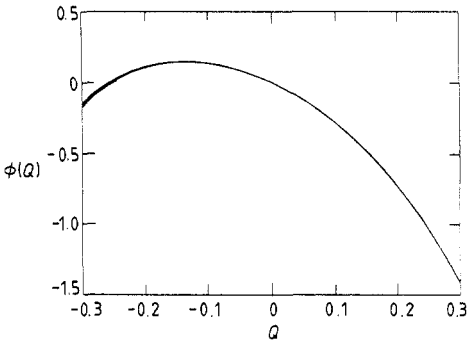

Figure 3. Plot of the amplitude $\Phi(Q)$ which characterises the scaling form of the exponent $\tau(Q)$, and of the related apparent $f(\alpha)$ curves, in the case of the abstract Fibonacci sequence. The plotted curves, corresponding to $18 \leqslant n \leqslant 28$, collapse in a very satisfactory way.

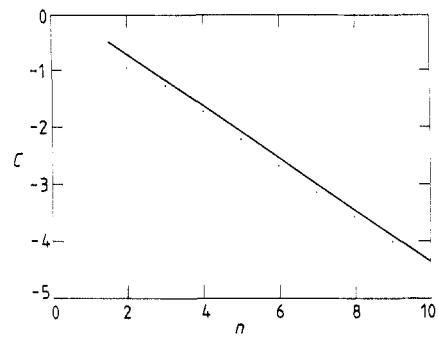

Figure 4. Plot of the curvature C of the apparent $f(\alpha)$ curves of the abstract circle sequence, against the generation label n. The straight line has a slope $s \approx -0.46$.

4.2. The circle sequence

We have mentioned in section 1 that the present study has been mostly motivated by a series of recent works [1-5], devoted to structures 'beyond quasiperiodicity', with either an unbounded density fluctuation [1-3], or a singular continuous Fourier intensity [4, 5]. Throughout these investigations, a central mathematical object was the following binary squence:

$$\varepsilon_n = \chi_\Delta(n\omega) \tag{4.5}$$

where ω and Δ are two arbitrary parameters, between 0 and 1, and χ_Δ denotes the characteristic function of the interval $[0;\Delta]$ on the circle, whence the name of the sequence. Equivalently, the multiples $n\omega$ of the 'frequency' ω are taken modulo unity. The binary quantity ε_n is thus equal to 1 (respectively 0) if the fractional part of $n\omega$ lies between 0 and Δ (respectively between Δ and 1).

The abstract circle sequence is easily shown to be quasiperiodic for any values of the parameters ω and Δ. The Fibonacci sequence is recovered in the special case $\omega = \Delta = \tau^{-2}$, where τ denotes the golden mean. More generally, whenever Δ assumes the form

$$\Delta = r\omega \mod 1 \tag{4.6}$$

where r is any integer, both the abstract sequence and the associated binary structure are quasiperiodic, and have a bounded fluctuation with respect to their average lattice.

For generic values of ω and Δ, when the 'Kesten condition' (4.6) is not satisfied, the density fluctuation is not bounded [13], and the Fourier transform of the binary structure has been conjectured to be singular continuous [4, 5], although that of the abstract sequence is quasiperiodic. The model therefore exhibits a change in the nature of the Fourier intensity when going from the sequence to the structural model. Among other phenomena, this instability is reminiscent of the transitions from quasiperiodic to chaotic motion that occur in some simple driven quantum systems.

The particular case defined by the values

$$\omega = \tau^{-2} \qquad \Delta = \tfrac{1}{2} \tag{4.7}$$

has been most studied, since it corresponds to the simplest of the self-similar sequences that are interesting, in the sense of not fulfilling the Kesten condition. This particular sequence, to be called simply the 'circle' sequence in the following, is generated by a substitution acting on three letters, namely

$$\sigma_C \begin{vmatrix} A \to CAC \\ B \to ACCAC \\ C \to ABCAC. \end{vmatrix} \tag{4.8}$$

The associated matrix

$$\mathbf{M} = \begin{pmatrix} 1 & 2 & 2 \\ 0 & 0 & 1 \\ 2 & 3 & 2 \end{pmatrix} \tag{4.9}$$

has a characteristic polynomial $P(\lambda) = (\lambda+1)(\lambda^2-4\lambda-1)$, which is not irreducible over the integers. The eigenvalues are τ^3, -1 and $-\tau^{-3}$. Since one eigenvalue has unit modulus, the circle sequence is a marginal case, with respect to the Bombieri–Taylor classification discussed in subsection 3.3.

The sequence ε_n of (4.5) is recovered by the identification

$$A : \varepsilon = 1 \qquad B : \varepsilon = 1 \qquad C : \varepsilon = 0. \tag{4.10}$$

In analogy with the Fibonacci sequence, we introduce the words A_n, B_n and C_n, obtained by acting n times with the substitution σ_C on the letters A, B and C. The Fourier amplitudes of the associated words for the abstract sequence are denoted by

g_n^A, g_n^B and g_n^C, whereas the amplitudes for the structural model are denoted by G_n^A, G_n^B and G_n^C. The first set of amplitudes obey the recursion relation

$$\begin{aligned} g_{n+1}^A &= g_n^C + \exp(-iq\nu_n^C)g_n^A + \exp[-iq(\nu_n^C + \nu_n^A)]g_n^C \\ g_{n+1}^B &= g_n^A + \exp(-iq\nu_n^A)g_n^C + \exp[-iq(\nu_n^A + \nu_n^C)]g_{n+1}^A \\ g_{n+1}^C &= g_n^A + \exp(-iq\nu_n^A)g_n^B + \exp[-iq(\nu_n^A + \nu_n^B)]g_{n+1}^A \end{aligned} \tag{4.11}$$

with the initial conditions

$$g_0^A = g_0^B = e^{-iq} \qquad g_0^C = 0. \tag{4.12}$$

The numbers of atoms of these words can be expressed in terms of the Fibonacci numbers, namely

$$\nu_n^A = F_{3n+1} \qquad \nu_n^B = \nu_n^C = F_{3n+2}. \tag{4.13}$$

The abstract circle sequence is quasiperiodic, with Bragg peaks for values of q in the same module (4.1) as the Fibonacci sequence, with the restriction that k is an odd integer. Hence the Fourier intensity of the circle sequence is also expected not to be a multifractal measure.

In order to check this lack of multifractality, we have still used the curvature C. Figure 4 shows a plot of this quanitity, for the Fourier transform of the words C_n, against the generation label n, up to $n = 9$. The word C_9 contains $F_{29} = 514\,229$ letters. An asymptotic linear growth of the curvature C with a slope $s \approx -0.46$, shown as a straight line on the plot, is clearly seen. Figure 5 shows a plot of the abscissa α_0 of the top of the $f(\alpha)$ curves, against $1/n$. Just as in the Fibonacci case, the data points converge to the limit value $\alpha_0 = 2$. A mechanism analogous to that described in subsection 4.1 can be expected to give rise to such a simple limit value.

We turn now to the more interesting case of the associated binary structural model, defined by associating two bond lengths to the letters, according to the rule

$$A: l = 1 + \xi \qquad B: l = 1 + \xi \qquad C: l = 1. \tag{4.14}$$

The Fourier amplitudes G_n^A, G_n^B and G_n^C obey recursion relations which are formally identical to (4.11), but with different initial values, namely $G_0^A = G_0^B = \exp[-iq(1+\xi)]$, $G_0^C = e^{-iq}$.

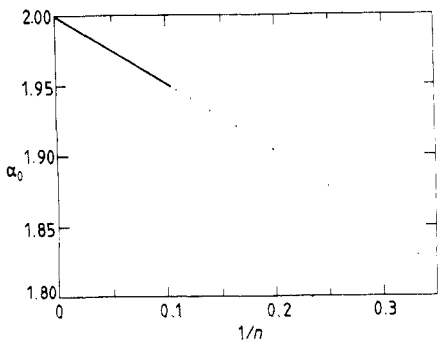

Figure 5. Plot of the abscissa α_0 of the top of the apparent $f(\alpha)$ curves for the abstract circle sequence, against the reciprocal of the generation label n. The limit value is $\alpha_0 = 2$.

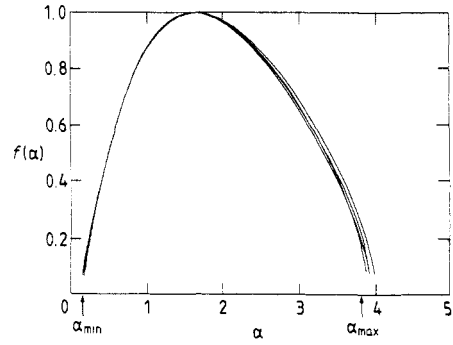

Figure 6. Plot of the $f(\alpha)$ curves associated with the structural model generated by the circle sequence. The plotted data correspond to the values $4 \leq n \leq 7$ of the generation label. The values of α_{min} and α_{max}, indicated by arrows, have been extracted from a vast amount of data, obtained with many different values of ξ and z.

We have been led to conjecture in previous works [4, 5], that the Fourier intensity is generically a purely SC measure. We may therefore expect a non-trivial $f(\alpha)$ curve in the limit of an infinite structure.

Let us emphasise the following point. The statistical properties of the Fourier transform of the binary structure associated with the circle sequence depend *a priori* on two parameters, namely the value of ξ, i.e. the ratio of both bond lengths, and the number z of 'Brillouin zones' that enter the computation, i.e. the range of wavevectors explored. Our goal has been rather ambitious, namely to determine whether the circle sequence possesses a universal $f(\alpha)$ curve, independently of both parameters ξ and z.

Figure 6 shows a plot of the $f(\alpha)$ curves for the words C_n, for $4 \leqslant n \leqslant 7$, and for $\xi = -\tau^2$ (the same value as for figure 1), and $z = 3$ 'zones'. Although the data vary with the generation n in a non-monotonic fashion, they tend to indicate convergence toward a limit smooth curve. We have repeated the numerical computation for many values of ξ, and up to $z = 10$ 'zones'. The behaviour shown in figure 6 is observed quite generically. The intrinsic scatter of the data decreases in a roughly systematic way when both n and z are increased. The vast amount of data in our possession suggests the existence of a well defined limit $f(\alpha)$ curve, attached to the circle sequence in an intrinsic way, independently of the parameters ξ and z. The extremal values $\alpha_{\min}$ and $\alpha_{\max}$ of the exponent α, around which the convergence of data is the worst, are indicated by arrows on the plot, and given below and in table 1. The observed poor convergence in the vicinity of the extremal values of the exponent α, corresponding to $f(\alpha) = 0$, is explained by means of the interpretation in terms of box counting. Indeed, (1.7) shows that the smaller $f(\alpha)$ is, the smaller the relevant number of boxes, or wavevectors. Fluctuation effects thus become more important in the 'tails' of the $f(\alpha)$ spectrum.

The structural model generated by the circle sequence is thus our first example of a genuine multifractal Fourier transform, with a non-degenerate $f(\alpha)$ curve. According to the discussion of subsection 3.4, the multifractality of a Fourier transform implies in particular that the following characteristic quantities assume non-trivial values, which have been extracted from our row data concerning many different values ξ and z:

$$\alpha_0 \approx 1.60 \qquad \alpha_{\min} \approx 0.15 \qquad \alpha_{\max} \approx 3.8 \qquad \alpha_1 \approx 0.55 \qquad d_P \approx 0.86. \tag{4.15}$$

This study can be put in perspective with respect to our previous works [4, 5]. The exponent β characterising the fall-off of the integral I_N, defined in (3.26), has been evaluated numerically in [4] to be $\beta = 0.16 \pm 0.04$. This quantity is related to the present multifractal formalism: it can indeed be argued that $\beta = \frac{1}{2}(1 - D_{1/2})$. Secondly, the local exponent α has been evaluated analytically in [5] for a dense but countable set of values of the wavevector q. The outcome turns out to depend in a continuous way on both q and ξ, and can assume any value between $\alpha = 0$ and $\alpha = 2$. Hence there is a countable set of values of q for which α is less than $\alpha_{\min}$. This is not too much of a paradox, since the multifractal analysis is a statistical and global approach, that may omit 'thin' (e.g. countable) sets with a vanishing dimension.

4.3. The Thue-Morse sequence

The Thue-Morse sequence is one of the most famous arithmetic sequences. It is a binary sequence ($\varepsilon_k = \pm 1$) defined as follows. Let s_k be the sum of the digits (0 or 1) of the representation of the integer $(k-1)$ in base two. Then the kth symbol ε_k of the sequence is 1 (respectively -1) if s_k is even (respectively odd). The Thue-Morse

sequence has been the subject of much mathematical activity (see [14] for a review). We have chosen to study the Thue-Morse sequence in the present context because of its conceptual simplicity, and the richness of the behaviour of its Fourier transform.

Among other possible definitions, the Thue-Morse sequence can be constructed by means of the following substitution, acting on two letters:

$$\sigma_{TM}\begin{vmatrix} A \to AB \\ B \to BA \end{vmatrix} \tag{4.16}$$

followed by the identification:

$$A : \varepsilon = 1 \qquad B : \varepsilon = -1. \tag{4.17}$$

Let A_n and B_n denote the words obtained by acting n times on the letters A and B with the substitution σ_{TM}. These words contain 2^n letters. The associated Fourier amplitudes g_n^A and g_n^B for the abstract sequence obey the recursion relations

$$g_{n+1}^A = g_n^A + \exp(-\mathrm{i}2^n q) g_n^B \qquad g_{n+1}^B = g_n^B + \exp(-\mathrm{i}2^n q) g_n^A \tag{4.18}$$

with the initial conditions

$$g_0^A = -g_0^B = \mathrm{e}^{-\mathrm{i}q}. \tag{4.19}$$

Owing to the symmetry of both the recursion relation (4.18) and the initial values (4.19), the Fourier amplitudes can be written explicitly in the form of finite products. The associated intensities (structure factors) are

$$S_n = 2^{-n}|g_n^A|^2 = 2^{-n}|g_n^B|^2 = \prod_{m=0}^{n-1} [2 \sin^2(2^{m-1}q)] \qquad n \neq 0. \tag{4.20}$$

These Fourier intensities can be shown (see, e.g., [15]) to obey a power law of the form (3.24) for every rational value of $x = q/(2\pi)$. Let us just state the results. Let $q = 2\pi j/k$, with j and k integers, and k odd. Then the sequence $2^{m-1}q \pmod{2\pi}$ of the phases entering the product in (4.20) is eventually periodic, with some period $p \leqslant k$. This means that there exists m_0 such that $2^{m+p}q = 2^m q \pmod{2\pi}$ for any $m \geqslant m_0$. It is then easy to derive from this observation the scaling law

$$S_n(2\pi j/k) \sim 2^{n(1-\alpha_{j/k})}. \tag{4.21}$$

This definition of the exponent α coincides with that of section 3, by virtue of (3.25). The explicit expression of the exponent is the following:

$$1 - \alpha_{j/k} = 2\gamma_{j/k} - 1 = \frac{1}{p \ln 2} \sum_{m=m_0+1}^{m=m_0+p} \ln[2 \sin^2(2^m \pi j/k)]. \tag{4.22}$$

It is then easy to realise that the same scaling law (4.21), with the same value of the exponent $\alpha_{j/k}$, also holds for any wavevector of the form $q = 2\pi(j/k + M)/2^N$, for any integers M and N ($N \geqslant 1$). The strongest of the local singularities, namely the smallest of the exponents α, occurs for $q = 2\pi/3$, and all the related values of the wavevector, where we have

$$\alpha_{1/3} = 2 - \frac{\ln 3}{\ln 2} \approx 0.415\,037. \tag{4.23}$$

The Fourier intensity therefore exhibits an infinity of different local exponents $\alpha_{j/k}$, ranging from $\alpha_{1/3}$ to ∞. It has been argued in [12, 15] that an infinity of those exponents are smaller than unity, and thus correspond to peaks.

The Fourier intensity measure of the Thue-Morse sequence also exhibits a dense set of essential singularities. In order to demonstrate this, we notice first that (4.20) implies the following functional equation for the intensities $S_n(q)$:

$$S_n(q) = 2\sin^2(q/2)S_{n-1}(2q). \tag{4.24}$$

It can be shown, by iterating (4.24), that the structure factors behave for small wavevector as $S_n(q) \sim 2^{n(n-2)}q^{2n}$. Hence the limit distribution function $H(q)$ vanishes more rapidly that any power of q near $q = 0$. In a more quantitative way, by requiring that the above estimate be stationary with respect to n, we obtain the following rough estimate:

$$H(q) = \exp\left(-\frac{(\ln q)^2}{\ln 2} + \mathcal{O}(\ln q)\right). \tag{4.25}$$

A similar essential singularity is also present at any dyadic value of the wavevector, of the form $q = 2\pi M/2^N$, for arbitrary integers M and N, with $N \geqslant 1$.

Let us now turn to the multifractal analysis of the Fourier intensity measure. According to the procedure described in subsection 3.4, we have to consider wavevectors of the form $q = 2\pi m/2^n$, with m ranging from 1 to 2^n, when dealing with the partial intensity S_n. Since the intensities are obviously even functions of q, and 2π-periodic, the range of m can be limited to 2^{n-1}. Moreover, (4.20) shows that S_n vanishes identically for even values of m. The vanishing of these amplitudes is somehow related to the essential singularities described above. We have therefore to adapt the definition (1.4) of the partition function $Z(Q)$, by restricting the sum to odd values of m, ranging from 1 to $2^{n-1}-1$, i.e. 2^{n-2} values of the wavevector, with an appropriate normalisation, namely

$$Z(Q) = \sum_m \left(2\prod_{k=0}^{n-1}\sin^2(2^{k-n}m\pi)\right)^Q. \tag{4.26}$$

For positive values of the parameter Q, the data (plotted in figure 7) converge very smoothly towards a limit $f(\alpha)$ curve. For any fixed negative value of Q, the data for α corresponding to the successive finite words go rapidly to infinity, roughly linearly in n. This phenomenon seems to be related to the presence of essential singularities

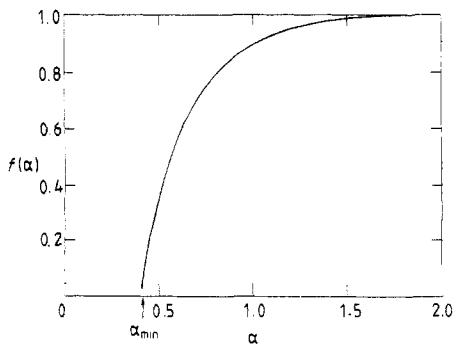

Figure 7. Plot of the left part of the $f(\alpha)$ curves associated with the abstract Thue-Morse sequence, for a generation label $10 \leqslant n \leqslant 16$. The lack of convergence of the right parts of the curves is commented on in the text.

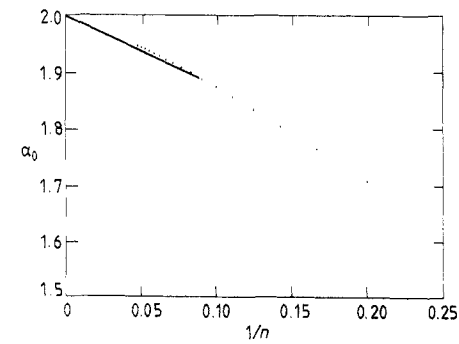

Figure 8. Plot of the abscissa α_0 of the top of the apparent $f(\alpha)$ curves for the abstract Thue-Morse sequence, against the reciprocal of the generation label n. The limit value is $\alpha_0 = 2$.

of the form (4.25) at dyadic value of the wavevector, since this dense set of points corresponds formally to a local exponent $\alpha = \infty$.

The Thue-Morse sequence therefore gives rise to 'half a multifractal spectrum'. The minimal value $\alpha_{\min}$ of the exponent α, corresponding to the $Q \to \infty$ limit, agrees, within the accuracy of the numerical work, with the value of the local exponent $\alpha_{1/3}$, given in (4.23)

$$\alpha_{\min} = \alpha_{1/3}. \tag{4.27}$$

We are thus facing a very favourable case, for which we have been able to identify which values of q have the local singularities corresponding to the exponent $\alpha = \alpha_{\min}$.

The abscissas α_0 of the tops of the $f(\alpha)$ curves of successive finite words are shown on figure 8, plotted against $1/n$, up to $n = 18$, i.e. $2^{18} = 262\,144$ letters. The data converge clearly linearly toward the limit value

$$\alpha_0 = 2. \tag{4.28}$$

As a matter of fact, this simple result can be derived analytically, by differentiating the partition function (4.26) appropriately.

The curvature C of the $f(\alpha)$ curves at their top, introduced in (2.4), is shown in figure 9, plotted against $1/n$. The numerical values exhibit a reasonably linear convergence toward a limit value $C \approx -0.07$. The left part of the $f(\alpha)$ spectrum is thus regular at its top, although this corresponds to an endpoint of the curve.

Finally, the other remarkable values associated with the multifractal spectrum are

$$\alpha_1 \approx 0.73 \qquad d_P \approx 0.89. \tag{4.29}$$

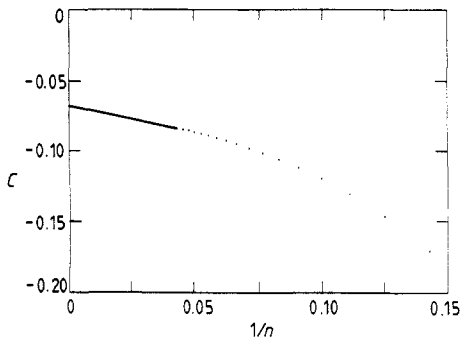

Figure 9. Plot of the curvature C of the $f(\alpha)$ curves of the Thue-Morse sequence at their top, against the reciprocal of the generation label n. A non-trivial limit value $C \approx -0.07$ shows up very clearly.

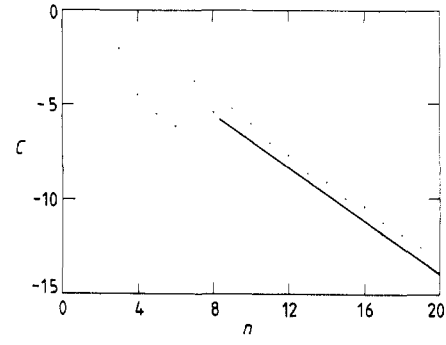

Figure 10. Plot of the curvature C of the apparent $f(\alpha)$ curves for the abstract Rudin-Shapiro sequence, against the generation label n. The straight line has the slope $s = -\ln 2$, derived in a heuristic way in the text.

4.4. The Rudin-Shapiro sequence

Just as with the Thue-Morse sequence studied in the last section, the Rudin-Shapiro sequence is a very well known object in the area of arithmetical sequences (see [14] for a review). Consider again the representation of the integer $(k-1)$ in base two, and let t_k be the number of times the string '11' shows up in this expansion. The kth term of the Rudin-Shapiro sequence is then $\varepsilon_k = 1$ (respectively $\varepsilon_k = -1$) if t_k is even

(respectively odd). One alternative definition of this binary sequence involves the following substitution, acting on four letters:

$$\sigma_{\mathrm{RS}} \left| \begin{array}{l} \mathrm{A} \to \mathrm{AC} \\ \mathrm{B} \to \mathrm{DC} \\ \mathrm{C} \to \mathrm{AB} \\ \mathrm{D} \to \mathrm{DB} \end{array} \right. \tag{4.30}$$

followed by the identification

$$A : \varepsilon = 1 \qquad B : \varepsilon = -1 \qquad C : \varepsilon = 1 \qquad D : \varepsilon = -1. \tag{4.31}$$

In analogy with the previous examples, we denote by $A_n, \ldots, D_n$ the words of length 2^n, produced by the action of n times the substitution on the initial letters, and by $g_n^A, \ldots, g_n^D$ the associated Fourier amplitudes for the abstract sequence. These quantities obey the recursion relations

$$\begin{aligned} g_{n+1}^A &= g_n^A + \exp(-\mathrm{i}2^n q) g_n^C \qquad & g_{n+1}^B &= g_n^D + \exp(-\mathrm{i}2^n q) g_n^C \\ g_{n+1}^C &= g_n^A + \exp(-\mathrm{i}2^n q) g_n^B \qquad & g_{n+1}^D &= g_n^D + \exp(-\mathrm{i}2^n q) g_n^B \end{aligned} \tag{4.32}$$

with the initial conditions

$$g_0^A = g_0^C = \mathrm{e}^{-\mathrm{i}q} \qquad g_0^B = g_0^D = -\mathrm{e}^{-\mathrm{i}q}. \tag{4.33}$$

It can be shown by induction on n, using (4.32), (4.33), that the Fourier amplitudes obey the following equalities: $g_n^A = -g_n^D$ and $g_n^B = -g_n^C$. There are thus only two independent amplitudes. This noticeable property allows one to rearrange the recursion equations obeyed by the associated Fourier intensities. These equations assume a simple form if we introduce three real quantities X_n, Y_n and Z_n, according to

$$\begin{aligned} & S_n^A = 2^{-n} |g_n^A|^2 = 1 + Z_n \qquad S_n^B = 2^{-n} |g_n^B|^2 = 1 - Z_n \\ & 2^{-n} g_n^A (g_n^B)^* = X_n + \mathrm{i} Y_n. \end{aligned} \tag{4.34}$$

In terms of these variables, we have the linear recursion formula

$$\begin{pmatrix} X_{n+1} \\ Y_{n+1} \\ Z_{n+1} \end{pmatrix} = \mathbf{O}_n \begin{pmatrix} X_n \\ Y_n \\ Z_n \end{pmatrix} \qquad \text{with } \mathbf{O}_n = \begin{pmatrix} 0 & 0 & -1 \\ \sin 2^n q & -\cos 2^n q & 0 \\ -\cos 2^n q & -\sin 2^n q & 0 \end{pmatrix} \tag{4.35}$$

together with the initial conditions $X_0 = -1$, $Y_0 = Z_0 = 0$. It can be checked that the matrices $\mathbf{O}_n$ are orthogonal ($\mathbf{O}_n^{\mathrm{t}} \mathbf{O}_n = \mathbf{1}$), and thus represent rotations in the three-dimensional XYZ Euclidean space. Since the initial point lies on the unit sphere, the whole sequence of points (X_n, Y_n, Z_n) also lies on the unit sphere. In particular, we have the inequality $|Z_n| \leqslant 1$, and therefore $0 \leqslant S_n \leqslant 2$, for all values of the generation label n, and of the wavevector q. In other words, the Fourier intensity is bounded, and no value of q can have a local exponent α less than unity.

Besides the rigorous results mentioned just above, (4.35) has suggested to us the following heuristic argument. For a generic value of q, and for n large, the point (X_n, Y_n, Z_n) is obtained from the initial point (X_0, Y_0, Z_0) through the action of a large number of non-commuting rotations, with generic angles. This observation suggests the possibility that, when the wavevector q is varied between 0 and 2π, the representative point is distributed uniformly over the unit sphere. If this assertion is true, it implies in particular that the third component Z_n is distributed uniformly over

the range $[-1; 1]$, and that the intensities S_n^A and S_n^B are distributed uniformly over the interval $[0; 2]$. We have checked this last statement numerically, taking, e.g., the equally spaced values of q dictated by the formalism of subsection 3.4. The uniform distribution of the intensities is verified in a very accurate fashion.

As a matter of fact, it is known in the mathematical literature (see, e.g., [14]) that the Fourier measure of the Rudin-Shapiro sequence is purely AC (abolutely continuous), the intensity associated with the infinite sequence being simply

$$S(q) = 1/(2\pi). \tag{4.36}$$

This value coincides with the average of the intensities S_n^A and S_n^B of the finite words, over the uniform distribution discussed just above, as it should.

The striking result (4.36) is equivalent to saying that the two-point correlation function $C(r)$ of the sequence vanishes identically, except for its value at coinciding points, namely

$$C(r) = \lim_{N\to\infty} \frac{1}{N} \sum_{n=1}^{N} \varepsilon_n \varepsilon_{n+r} = \delta_{r,0} \tag{4.37}$$

where δ on the right-hand side stands for Kronecker's symbol.

Let us now turn to the multifractal analysis of the Fourier intensity. Figure 10 shows the numerical values of the curvature C of the $f(\alpha)$ curves at their top, calculated from the intensities S_n^A, and plotted against the generation label n, up to $n = 20$, i.e. $2^{20} = 1048\,576$ letters. A very clear linear behaviour can be seen, thus confirming our expectation, namely the lack of multifractality.

The observed linear growth of the curvature C as a function of the generation label n can be checked as follows. We have argued that the intensity $S_n^A(q)$ is distributed, for n large enough, uniformly over the interval $[0; 2]$. We are therefore in the situation of the example introduced in section 2, in order to illustrate finite-size effects. The uniform distribution over $[0; 2]$ plays the part of $g(x)\,dx$. We can therefore use (2.5), which leads to the estimate $C \approx -n \ln 2$ in the present case. A straight line with slope $s = -\ln 2$ has been drawn on figure 10. The data agree with this heuristic prediction in a very satisfactory way.

4.5. Examples of non-PV substitutions

This last section is devoted to generic substitutions, that do not have the PV property, discussed in subsection 3.3. More precisely, we also exclude from the present analysis the marginal cases where the second largest eigenvalue lies on the unit circle, and require that the substitution has two eigenvalues strictly larger than unity in modulus, in such a way that the density fluctuation diverges with a positive exponent δ, defined in (3.34).

The following two examples of substitutions acting on two and three letters, respectively, do not have any particular physical or arithmetic origin, but have, rather, been chosen according to a natural criterion of minimality, to be explained below.

4.5.1. The binary case. Consider a general binary substitution (acting on two letters). The associated 2×2 matrix $\mathbf{M}$ has non-negative integer entries. Its characteristic polynomial is $P(\lambda) = \det(\lambda \mathbf{1} - \mathbf{M}) = \lambda^2 - s\lambda + p$, where $s = \operatorname{tr} \mathbf{M}$ and $p = \det \mathbf{M}$ are the invariants of the matrix. Let λ_1 and λ_2 denote the eigenvalues of $\mathbf{M}$. In virtue of the Perron-Frobenius theorem, the root with largest modulus, say λ_1, is real, and larger

than 1. The other root is then also real. We are thus left with two classes of binary non-PV substitutions, namely the following.

(i) $\lambda_2 < -1 < 1 < \lambda_1$. This occurs for $s \geqslant 1$, and $p \leqslant -s-2$. The minimal example (with the smallest possible value of λ_1) corresponds to $s=1$ and $p=-3$, yielding $\lambda_{1,2} = \frac{1}{2}(1 \pm \sqrt{13}) \approx (2.302\,78, -1.302\,78)$.

(ii) $1 < \lambda_2 < \lambda_1$. This occurs for $s \leqslant p < s^2/4$, implying in particular $s \geqslant 5$. The minimal solution $s=p=5$ yields $\lambda_{1,2} = \frac{1}{2}(5 \pm \sqrt{5}) \approx (3.618\,03, 1.381\,97)$.

The minimal non-PV subsitution acting on two letters, in the sense that its Perron-Frobenius eigenvalue λ_1 is the smallest, corresponds therefore to the minimal solution of the first class, namely $s=1$ and $p=-3$. The associated eigenvalues, quoted just above, lead to a fluctuation exponent $\delta \approx 0.317\,10$. It is easily realised that there are only two substitutions, up to letter permutations, which correspond to these values of the invariants. One of these substitutions is

$$\sigma_2 \left| \begin{array}{l} A \to AB \\ B \to AAA. \end{array} \right. \tag{4.38}$$

In the following, we focus our attention on this example.

We define a numerical binary sequence by means of the identification

$$A : \varepsilon = 1 \qquad B : \varepsilon = -1. \tag{4.39}$$

We introduce the words A_n and B_n, obtained by acting n times with σ_2 on the letters A and B. The numbers of letters ν_n^A and ν_n^B of these words obey the recursion relation

$$\nu_{n+1}^A = \nu_n^A + \nu_n^B \qquad \nu_{n+1}^B = 3\nu_n^A \tag{4.40}$$

with the initial condition $\nu_0^A = \nu_0^B = 1$. The associated Fourier amplitudes of the abstract sequence are given by the following recursion relations:

$$\begin{aligned} g_{n+1}^A &= g_n^A + \exp(-\mathrm{i}q\nu_n^A) g_n^B \\ g_{n+1}^B &= [1 + \exp(-\mathrm{i}q\nu_n^A) + \exp(-2\mathrm{i}q\nu_n^A)] g_n^A \end{aligned} \tag{4.41}$$

with the initial conditions $g_0^A = -g_0^B = \mathrm{e}^{-\mathrm{i}q}$.

Let us emphasise that this example is the first one for which nothing is known, on a rigorous basis, about the nature of the Fourier intensity measure, except for the BT argument, which tells us that there should be no atomic component (Bragg peaks).

We have performed the multifractal analysis of the Fourier intensity measure of the abstract sequence generated by σ_2. Figure 11 shows a plot of the left parts of the $f(\alpha)$ curves, corresponding to positive values of the parameter Q, for the words B_n, with a generation label n ranging from 11 to 14. The largest word has $\nu_{14}^B = 140\,694$ letters. Although the data converge in a rather slow and non-monotonic way, there seems to exist a well defined limit curve. For negative values of Q, the data for α diverge roughly linearly with the generation label n, just as in the case of the Thue-Morse sequence. We attribute this lack of convergence to the possible existence of essential singularities in the integrated intensity $H(q)$, analogous to those of (4.25). We have checked carefully that the abscissae of the $f(\alpha)$ curves at their top exhibit a smooth $1/n$ convergence towards the limit value $\alpha_0 = 2$, and the curvature C approaches a finite limit. The situation is therefore altogether very analogous to that of the Thue-Morse sequence.

The characteristic values extracted from the numerical data are summarised below

$$\alpha_0 = 2 \qquad \alpha_{\min} \approx 0.15 \qquad \alpha_1 \approx 0.44 \qquad d_{\mathrm{P}} \approx 0.83. \tag{4.42}$$

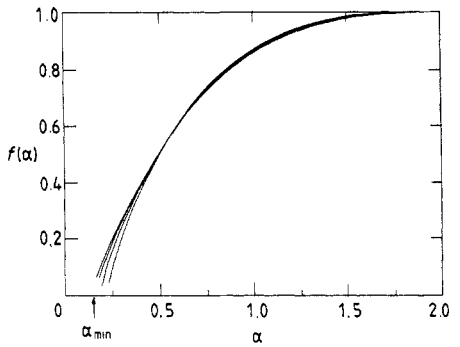

Figure 11. Plot of the left part of the $f(\alpha)$ curves associated with the words B_{11}-B_{14} of the abstract minimal non-PV binary sequence, defined in (4.38). The right halves of the curves do not converge. The value of $\alpha_{\min}$, indicated by an arrow, has been extracted from data concerning all generations, up to $n = 14$.

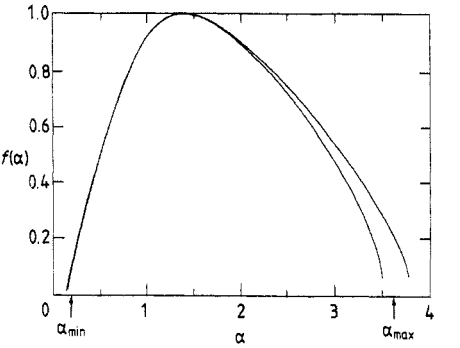

Figure 12. Plot of the $f(\alpha)$ curves corresponding to the words B_{27} and B_{31} of the abstract minimal non-PV ternary sequence, defined in (4.43). The values of $\alpha_{\min}$ and $\alpha_{\max}$, indicated by arrows, have been extracted from data concerning all generations, up to $n = 31$.

4.5.2. The ternary case. Consider now a generic ternary substitution (acting on three letters). The associated 3×3 matrix **M** has non-negative integer entries. Its characteristic polynomial $P(\lambda) = \det(\lambda \mathbf{1} - \mathbf{M}) = \lambda^3 - s\lambda^2 + t\lambda - u$ now involves three invariants, s, t and u.

In analogy with the binary case, we search for the values of these integer invariants, such that the largest eigenvalue λ_1 is real and larger than unity, and that there is at least another eigenvalue greater than unity in modulus. Moreover, we are mostly interested in the minimal ternary substitution, namely that with the smallest λ_1. The situation is much more involved than the binary problem, studied in subsection 4.5.1, where two classes of non-PV substitutions could be characterised. No analogous classification is known in the present case. The minimal non-PV substitution can nevetheless be determined as follows. If we assume that the Perron-Frobenius eigenvalue λ_1 is less than some bound R, then the invariants have to obey the inequalities $0 \leq s \leq 3R$, $|t| \leq 3R^2$ and $|u| \leq R^3$. These conditions leave only a finite number of possibilities, that can be enumerated by a simple computer program.

It turns out that the two solutions with the smallest values of λ_1 are the following: (i) $s = 1$, $t = 1$, and $u = 2$, yielding $\lambda_1 \approx 1.353\,21$, and (ii) $s = 0$, $t = -1$, and $u = 2$, yielding $\lambda_1 \approx 1.521\,38$. It is easy to realise that the first solution cannot represent the characteristic polynomial of a substitution matrix.

The minimal ternary example is therefore number (ii). We will focus our attention on one of the associated substitutions, defined by

$$\sigma_3 \begin{cases} A \to C \\ B \to A \\ C \to BAB. \end{cases} \tag{4.43}$$

The eigenvalues of the corresponding matrix are $\lambda_1 \approx 1.521\,38$, and $\lambda_{2,3} \approx -0.760\,69 \pm 0.857\,87$ i, so that the fluctuation exponent is $\delta \approx 0.325\,93$. This example is the first case where the substitution matrix has non-real eigenvalues.

We define a numerical binary sequence by means of the following identification:

$$A : \varepsilon = 1 \qquad B : \varepsilon = 1 \qquad C : \varepsilon = -1. \tag{4.44}$$

The substitution σ_3 shares with the Fibonacci substitution the property that it can be rewritten in terms of one single sequence of words. Indeed, if we denote by A_n, B_n and C_n the words defined in the usual way, the form (4.43) of σ_3 implies $A_n = B_{n+1}$ and $C_n = B_{n+2}$. It is therefore sufficient to consider the sequence of words B_n. Let ν_n be the number of letters of B_n, and g_n denote the corresponding partial Fourier amplitude for the abstract sequence. These quantities obey the following four-term recursion relations:

$$B_{n+3} = B_n B_{n+1} B_n \tag{4.45}$$

$$\nu_{n+3} = 2\nu_n + \nu_{n+1} \tag{4.46}$$

$$g_{n+3} = \{1 + \exp[-iq(\nu_n + \nu_{n+1})]\} g_n + \exp(-iq\nu_n) g_{n+1} \tag{4.47}$$

with the initial conditions $\nu_0 = \nu_1 = \nu_2 = 1$, $g_0 = g_1 = -g_2 = e^{-iq}$.

Let us now turn to the multifractal analysis of the Fourier intensity measure. Figure 12 shows a plot of the $f(\alpha)$ curves corresponding to the words B_n, for the values 27 and 31 of the generation label n. The larger sample has $\nu_{31} = 287\,867$ letters. The plot presents only two curves, for the sake of readability. The data converge indeed in a non-monotonic way to a rather well defined limit $f(\alpha)$ curve. The extremal values $\alpha_{\min}$ and $\alpha_{\max}$ have been extrapolated from data concerning all values of n, up to $n = 31$. We end this section by listing the following characteristic values:

$$\alpha_0 \approx 1.36 \qquad \alpha_{\min} \approx 0.2 \qquad \alpha_{\max} \approx 3.6 \qquad \alpha_1 \approx 0.64 \qquad d_P \approx 0.92. \tag{4.48}$$

5. Conclusion

In this paper it has been proposed to use multifractal analysis in reciprocal space, in order to obtain novel information concerning the global behaviour of the Fourier transform of a structural model. In elaborating this approach, we aimed more specifically at a better understanding of the structures introduced in our previous works. Indeed, from an intuitive viewpoint, those structures exhibit a possible intermediate kind of ordered matter, between (quasi)-periodicity and amorphousness.

The nature of the Fourier transform of these models is therefore the natural question to be answered, and the most precise context for doing so is the measure-theoretical one. As recalled in section 1, a Fourier intensity can be either atomic (Bragg peaks), AC (diffuse scattering), SC ('singular scattering'), or a superposition of any of these three pure types of measures. The Bombieri-Taylor argument is a very efficient tool for characterising which structures will 'diffract', i.e. possess Bragg peaks. The present study was partly motivated by the search of a counterpart of the BT argument, which would tell us whether a structure possesses diffuse scattering, i.e. an AC component in its Fourier transform.

By means of several examples of one-dimensional self-similar sequences and structures, generated by substitutions on finite alphabets, we have accumulated a good deal of experience concerning these matters. Table 1 presents a synthetic comparison between the results of our multifractal analysis of the Fourier transforms of the models, and information available from other sources. Table 1 also gives the numerical values of several characteristic quantities—when available—which are of special interest when dealing with the $f(\alpha)$ curve associated with a Fourier transform. Let us emphasise again the special role played by α_0, the abscissa of the top of the curve, to be interpreted as the strength of the singularitiy observed for a generic wavevector q, as well as d_P,

which represents the dimension of the set of peaks of the Fourier transform—in the general sense of singular scattering.

As a general rule, it turns out that our expectations concerning the multifractality of Fourier transforms are confirmed. Namely, both the atomic Fourier transforms, made of Bragg peaks, of periodic (quasiperiodic, almost-periodic) structures, and the AC Fourier transforms (diffuse scattering) correspond to degenerate $f(\alpha)$ curves, consisting of one or two isolated points. Conversely, the structures for which our numerical analysis leads undoubtedly to a non-trivial multifractal $f(\alpha)$ curve certainly exhibit only 'singular scattering': their Fourier transform is a purely SC measure.

The results summarised just above lead us therefore to formulate, as a kind of conclusion, the following two heuristic assertions. (a) Multifractal analysis in reciprocal space yields generically a non-trivial $f(\alpha)$ curve only when the Fourier intensity measure is SC, and corresponds to 'singular scattering'. (b) Self-similar structures have generically a non-trivial $f(\alpha)$ curve only when the substitution which defines the 'inflation rules' of the model does not have the PV property (namely, the second largest eigenvalue of the substitution matrix is larger than unity in modulus).

These conclusions have been presented on purpose as heuristic 'rules of thumb', which hold in any practical situation, but which probably cannot be turned into rigorous theorems. Indeed, leaving the realm of Fourier transforms, it has been argued that one can construct positive measures with essentially any kind of pathology with respect to multifractal analysis [16], such as, e.g., AC measures with a hierarchically built unbounded density, which have a non-trivial $f(\alpha)$ curve.

Acknowledgments

It is a pleasure for us to thank S Aubry, P Collet and P Moussa for very stimulating discussions on multifractality and related matters, and R Peschanski for a careful reading of the manuscript.

References

[1] Aubry S and Godrèche C 1986 *J. Physique Coll.* **C3** 187
[2] Aubry S, Godrèche C and Vallet F 1987 *J. Physique* **48** 327
[3] Godrèche C, Luck J M and Vallet F 1987 *J. Phys. A: Math. Gen.* **20** 4483
[4] Aubry S, Godrèche C and Luck J M 1987 *Europhys. Lett.* **4** 639
[5] Aubry S, Godrèche C and Luck J M 1988 *J. Stat. Phys.* **51** 1033
[6] Paladin G and Vulpiani A 1987 *Phys. Rep.* **156** 147
[7] Feder J 1988 *Fractals* (New York: Plenum)
[8] Bombieri E and Taylor J E 1986 *J. Physique Coll.* **C3** 19; 1987 *Contemp. Math.* **64** 241
[9] Pisot C 1938 *Ann. Scuola Norm. Sup. Pisa* **7** 205
Cassels J W S 1957 *An Introduction to Diophantine Aprpoximation* (Cambridge: Cambridge University Press)
[10] Dumont J M 1990 *Number Theory and Physics* ed J M Luck, P Moussa and M Waldschmidt (*Springer Proceedings in Physics* **47**) (Berlin: Springer)
[11] Godrèche C and Oguey C 1990 *J. Physique* **51** 21
[12] Luck J M 1989 *Phys. Rev.* B **39** 5834
[13] Kesten H 1966 *Acta Arith.* **12** 193
[14] Queffélec M 1987 *Substitution Dynamical Systems: Spectral Analysis* (*Lecture Notes in Mathematics* **1294**) (Berlin: Springer)
[15] Cheng Z, Savit R and Merlin R 1988 *Phys. Rev.* B **37** 4375
[16] Collet P unpublished